TISSUE ENGINEERING: Part C
Volume 00, Number 00, 2024

DOI: 10.1089/ten.tec.2024.0117

termis
Tissue Engineering
& Regenerative Medicine
International Society

Open camera or QR reader and scan code to access this article and other resources online.

METHODS ARTICLE

Misleading Pore Size Measurements in Gelatin and Alginate Hydrogels Revealed by Confocal Microscopy

Alexis Franco,[1,2] Bo Van Durme,[2] Sandra Van Vlierberghe,[2] and Christine Dupont-Gillain, PhD[1]

It is a well-documented phenomenon that the porous structure of hydrogels observed with vacuum-based imaging techniques is generated during the freezing and drying process employed prior to observation. Nevertheless, vacuum-based techniques, such as scanning electron microscopy (SEM), are still being commonly used to measure pore sizes in hydrogels, which is often not representative of the actual pore size in hydrated conditions. The frequent underestimation of the impact of freezing and drying on hydrogel structures could stem from a lack of cross-fertilization between materials science and biomedical or food science communities, or from the simplicity and visually appealing nature of SEM imaging, which may lead to an overemphasis on its use. Our study provides a straightforward and impactful way of pinpointing this phenomenon exploiting two hydrogels ubiquitously applied in tissue engineering, including gelatin methacryloyl and alginate as proof-of-concept hydrogels. By comparing images of the samples in the native hydrated state, followed by freezing, freeze-drying, and rehydration using SEM and confocal microscopy, we highlight discrepancies between hydrogel pore sizes in the hydrated versus the dry state. To conclude, our study offers recommendations for researchers seeking insight in hydrogel properties and emphasizes key factors that require careful control when using SEM as a characterization tool.

Keywords: hydrogel, structure, pore size, gelatin, alginate

Impact Statement

We demonstrate that tissue engineers should cease to use electron microscopies to characterize their native hydrogel structures, as they are only measuring freezing artifacts. Furthermore, researchers can now get more accurate insights on their hydrogel structure using confocal microscopy in the hydrated state.

Introduction

Hydrogels, that is, biphasic materials made of three-dimensional networks of hydrophilic polymers in water, have emerged as promising materials in various fields, particularly in tissue engineering, owing to their biocompatibility and ability to mimic the extracellular matrix. Vacuum-based imaging techniques, notably scanning electron microscopy (SEM), have been widely used to gain insight in the structures of hydrogels. However, it is well-documented that the porous structures observed in SEM images are often not intrinsic to the hydrogel matrix but are instead generated during the freeze-drying process.[1–4] Despite this well-established knowledge, vacuum-based techniques continue to be widely employed for pore size measurements in hydrogels. Their misuse leads to potentially misleading

[1]Bio and Soft Matter, Institute of Condensed Matter and Nanosciences, Université catholique de Louvain, Louvain-la-Neuve, Belgium.
[2]Polymer Chemistry and Biomaterials Group, Centre of Macromolecular Chemistry, Ghent University, Ghent, Belgium.

conclusions in published research. A disconnection between materials science and biomedical science communities could be a contributing factor to the underestimation of the artifacts generated by freezing and freeze-drying. The simplicity and visually appealing nature of SEM images could overshadow its inherent artifacts, potentially leading to an overemphasis on its application in pore size characterization.

In the native hydrated state, the porosity of hydrogels manifests itself at the scale of the mesh size of their polymer network, typically within the range of tens of nanometers.[5] As the hydrogels are frozen, supercooled water undergoes nucleation, and then the ice crystals grow into larger grains, as polymer chains are excluded from the ice crystals.[1] By the end of the freezing process, these ice grains reach sizes orders of magnitude greater than the original hydrogel mesh sizes. The ice grains are sublimated during the freeze-drying process, leaving the dry porous structure behind that is often imaged with SEM. The size of these pores largely depends on the ice formation kinetics. As the cooling rate increases, the frequency of ice undergoing primary nucleation also rises, resulting in a greater number of smaller pores in the freeze-dried structure.[2] By tinkering with the freezing conditions, various groups have shown that pores generated in the hydrogels can range from nanometers up to hundreds of micrometers.[2,4] The morphology of these pores can even be tuned by applying cooling rate gradients.[2] These phenomena are leveraged to generate custom porous scaffolds serving various applications.[6–8]

However, some articles report on the characterization of the porous structure of hydrogels exploiting SEM, while those pores would actually not exist in the native hydrated state.[9–13] It is often stated that a given pore size is needed for cells to be able to invade a hydrogel, this size being at the microscale.[13] Furthermore, even when freezing or freeze-drying is used intentionally to generate porous scaffolds, the methods frequently lack critical details regarding reproducibility, and assumptions are made about what becomes of these pores when the scaffold is rehydrated. Our study aims to bridge this gap by visually demonstrating the discrepancies between hydrogel structures in the hydrated state and those observed under vacuum conditions induced by freeze-drying. By focusing on two widely used hydrogels in tissue engineering, that is, gelatin methacryloyl (GelMA) and alginate, we aim to facilitate the dissemination of knowledge toward researchers less inclined to focus on fundamental materials science.

By comparing images of the hydrogel microstructures in different states (native hydrated, frozen at different cooling rates, freeze-dried, and rehydrated), we aim to provide a straightforward visualization strategy (Fig. 1) regarding freeze-drying-induced artifacts along with their impact on pore size measurements. Specifically, the microstructures of hydrogels are imaged in the hydrated state using confocal microscopy, before and after a freezing step to illustrate the impact of freezing (Result 1). Furthermore, the freeze-dried scaffolds imaged using SEM are compared with confocal microscopy images of the resulting scaffolds after rehydration to pinpoint the discrepancies between the two states (Result 2). Finally, freeze-dried scaffolds frozen using either a freezer or liquid nitrogen are compared to highlight the importance of cooling rate (Result 3).

Materials and Methods

GelMA synthesis

Gelatin methacrylamide, with a degree of substitution of 96% with respect to the primary amines, was obtained using a protocol described previously.[14,15] Briefly, gelatin was dissolved in a phosphate buffer at 40°C, followed by the addition of methacrylic anhydride (2.5 times the equivalent molar quantity of free primary amines present in gelatin). The reaction mixture was stirred for 1 h. Afterward, the solution was dialyzed for 24 h at 40°C against demineralized water. After dialysis, the pH of the solution was adjusted to 7.4 using NaOH, transferred to Petri dishes, and freeze-dried for later use.

GelMA hydrogels

A 10% (w/v) gelatin methacrylamide solution was prepared and 2 mol% (with respect to the methacryloyl groups present) of lithium phenyl-2,4,6-trimethylbenzoylphosphinate photoinitiator was added to the solution. The mixture was then poured into a 1-mm thick sheet mold and left to gelify at 4°C for 1 h. Then, photocrosslinking was performed under an ultraviolet lamp (365 nm, 4 W lamp) for 30 min. After unmolding, these gelatin sheets were stored in phosphate buffered saline (pH = 7.4, 140 mM sodium chloride, 2.68 mM potassium chloride, and 10 mM phosphate, prepared from tablets purchased from Gibco).

Alginate hydrogels

To obtain homogeneous alginate gels, the well-known slow gelation strategy was adapted from Sardelli *et al.*[16] Specifically, a 3 wt. % sodium alginate solution (A2033, medium viscosity, Sigma-Aldrich) was mixed with a 2 wt. % suspension of calcium carbonate (398101, Sigma-Aldrich) and with a 7 wt. % solution of Glucono delta-lactone (G4750, Sigma-Aldrich) at a 5:1:1 volume ratio. The mixture was poured into a 1-mm thick sheet mold and left for 24 h in the fridge for gelation. After unmolding, these alginate sheets were stored in a 0.1 wt. % calcium chloride solution.

Sample preparation

For imaging of hydrogels in the native hydrated state, the 1-mm thick pieces of hydrogel were directly observed with confocal microscopy. The hydrogels to be observed after

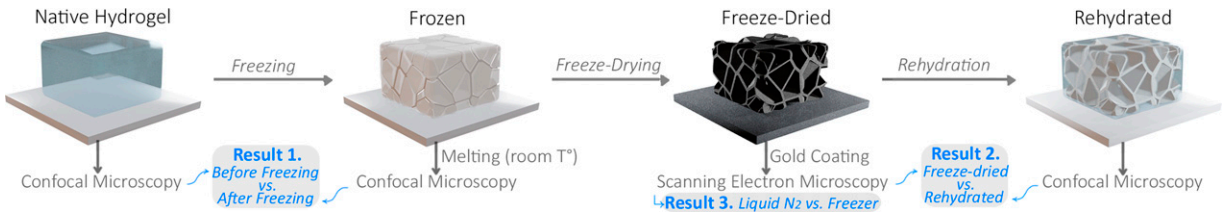

FIG. 1. Experimental design flowchart.

freezing were plunged into liquid nitrogen, and then put back into their storage solution prior to imaging via confocal microscopy. For freeze-drying, hydrogels were plunged into liquid nitrogen inside the chamber of a Christ Alpha 1-2 freeze-dryer and subsequently freeze-dried for 24 h. These samples were observed either in the dry state using SEM or in rehydrated state in their storage solution at room temperature using confocal microscopy. The rehydrated samples were kept in their storage solution for 4 h at least prior to observation. Note that hydrogel samples dried without freezing were not considered for imaging, as this leads to the full collapse of their structure, leading to a solid homogeneous mass.

Confocal microscopy

The samples were observed using their native autofluorescence, therefore, no dyes were used, ensuring no change in hydrogel structure related to labeling. For gelatin, the best results were achieved with shorter wavelengths, that is, a 400 nm laser. For alginate, similar imaging quality was obtained using lasers with wavelengths ranging from 400 to 600 nm. Therefore, all images were captured using 400 nm excitation laser.

SEM

Dry samples were carefully sliced in half using a sharp scalpel in order to observe the cross-section and not the surface "skin" of freeze-dried hydrogels. The section was sputtered with gold until a thickness of 15 nm was achieved. The imaging conditions of the JEOL 7600F scanning electron microscope were set to an acceleration voltage of 2 kV and a working distance of 15 mm.

Pore size measurements

For SEM and confocal microscopy, images for pore size measurements were captured in the bulk of the material, in areas where the structure was homogeneous across the field of view. This was to avoid the effect of the cooling rate gradients near the edge of the materials. A custom Python script was made to streamline data analysis using the open-source computer vision library (opencv-python). The images were passed through a manually adjusted binary threshold value to define pore areas (cv2.threshold). Edge detection was used to discriminate each individual pore (cv2.findContours). For each pore contour, the minimal area bound rectangle was fitted (cv2.minAreaRect) and its shortest dimension was defined to be the minimal pore diameter. More details regarding image analysis is given in Supplementary Data S1. Measurements were then compared using mean and standard deviation by Student's two-sample *t* test.

Experiments

Effect of freezing on the structure of gelatin and alginate hydrogels

Figure 2 shows confocal microscopy images of both gelatin and alginate hydrogel structures before and after being frozen in liquid nitrogen. Hydrogel samples were observed in their storage media at room temperature.

In both systems, before freezing, the images show no evidence of pores on the microscale in the native hydrated hydrogels. The images display a homogeneous fluorescence signal from all the surveyed area, apart from some impurities that have been kept in the frame to verify focus and resolution.

After freezing, new porous structures have appeared. In gelatin, these features have the appearance of cracks, whereas

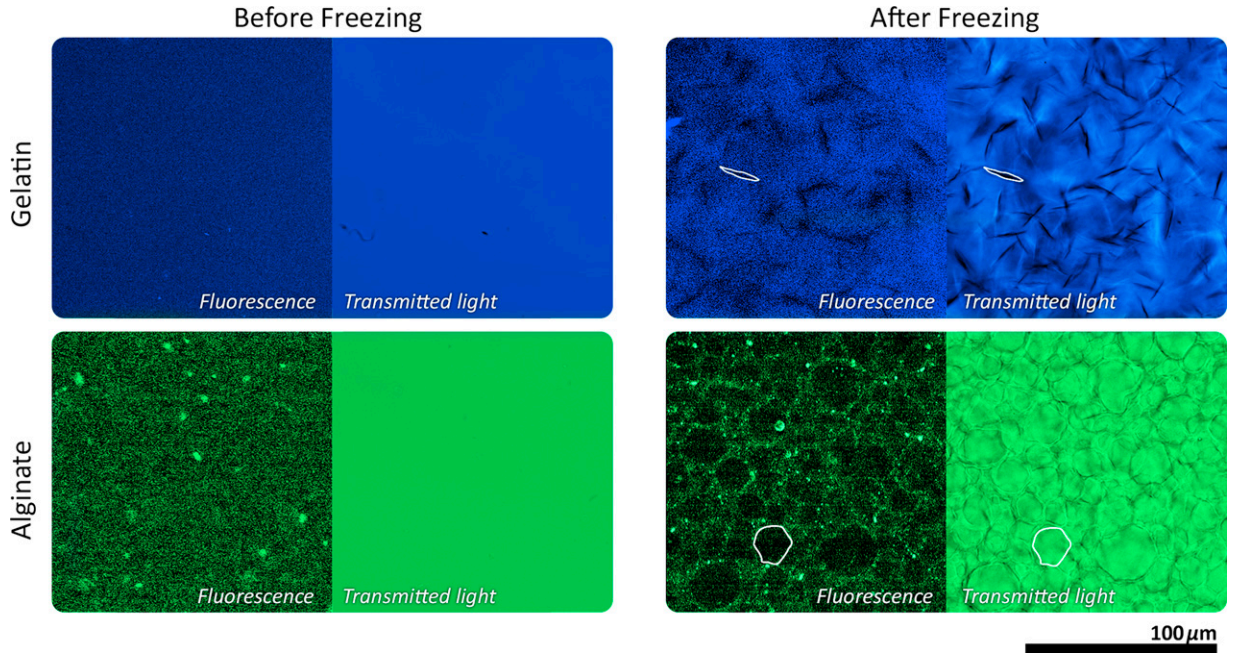

FIG. 2. Confocal microscopy images (fluorescence and transmitted light) of gelatin (*top*) and alginate (*bottom*) hydrogels before (*left*) and after (*right*) a freezing cycle. All images are shown at equal scale. All gels are observed at room temperature in their storage solutions. A representative pore is highlighted in white.

in alginate, these features have the appearance of globular pores. By fitting a bounding rectangle to the pore contours, the pore dimensions were measured being on average 30 ± 19 μm maximal and 9.7 ± 8.9 μm minimal diameter in gelatin and on average 38 ± 14 μm maximal and 31 ± 10 μm minimal diameter in alginate.

Effect of rehydration on freeze-dried gelatin and alginate hydrogels

Figure 3 shows SEM images of cross-sections of both gelatin and alginate hydrogels, confocal microscopy images of the freeze-dried hydrogels after being rehydrated, and a comparison of the measured pore sizes in the freeze-dried and rehydrated states for both systems.

When transitioning to the rehydrated state, a notable transformation is observed in gelatin hydrogels, where the pores shift from being round or elliptical toward flattened "cracks." In contrast, the pore morphology in alginate hydrogels remains consistent between the freeze-dried and rehydrated states.

Bar graphs representing the average minimal pore diameter, along with their associated standard deviations, provide a quantitative perspective. In the case of gelatin, there exists a significant reduction in pore size upon rehydration compared with the freeze-dried state ($p < 0.001$). However, for alginate, no notable difference is discerned between these two states.

Effect of cooling rate on pore size

Figure 4 compares SEM images of cross-sections of both gelatin and alginate hydrogels, when frozen by plunging into liquid nitrogen or left in a −25°C freezer, before freeze-drying.

The two systems show a tremendous difference in pore size depending on the applied freezing method. The liquid nitrogen frozen samples, which have been submitted to a much faster decrease in temperature, exhibit pore dimensions mostly below 100 μm. The maximal pore dimensions of the freezer samples approach the thickness of the samples themselves (1 mm).

Bar graphs represent the average minimal pore diameter, along with their associated standard deviations. A significant increase in minimal pore diameter ($p < 0.001$) is observed for both systems and is associated with the much lower cooling rate in the freezer.

Discussion

Pore size measurements in native hydrated hydrogels

The results obtained from confocal microscopy images of gelatin and alginate hydrogels before and after applying a freezing cycle (see Fig. 2) are instrumental in understanding the impact of freezing on the structural characteristics of these hydrogels. In the native hydrated state, both gelatin and alginate hydrogels exhibited a homogenous fluorescent signal without any discernible pores at the microscale. However, a freezing cycle led to the emergence of new structural porous features in both systems. Moreover, it becomes evident from these results that pore size measurements in SEM should not be used to infer properties of the native hydrated gel, as the pores observed in SEM do not exist before freezing.

This observation aligns with the expected behavior, as in the native hydrated state, the porosity of hydrogels typically manifests at the scale of their polymer networks' mesh size, which is in the range of nanometers, being far below the resolution of confocal microscopy owing to the diffraction

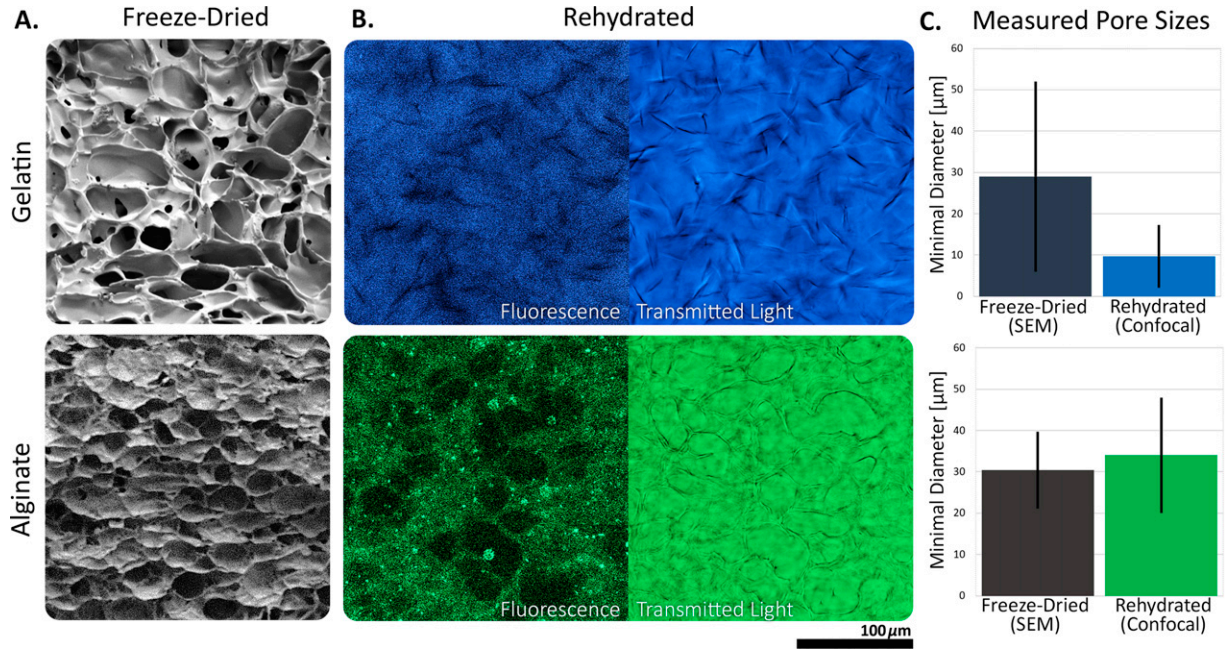

FIG. 3. **(A)** SEM micrographs of freeze-dried hydrogels and **(B)** confocal microscopy images of rehydrated hydrogels for gelatin (*top*) and alginate (*bottom*). All images are shown at equal scale. **(C)** Bar graphs show average minimal pore diameters ± standard deviation. SEM, scanning electron microscopy.

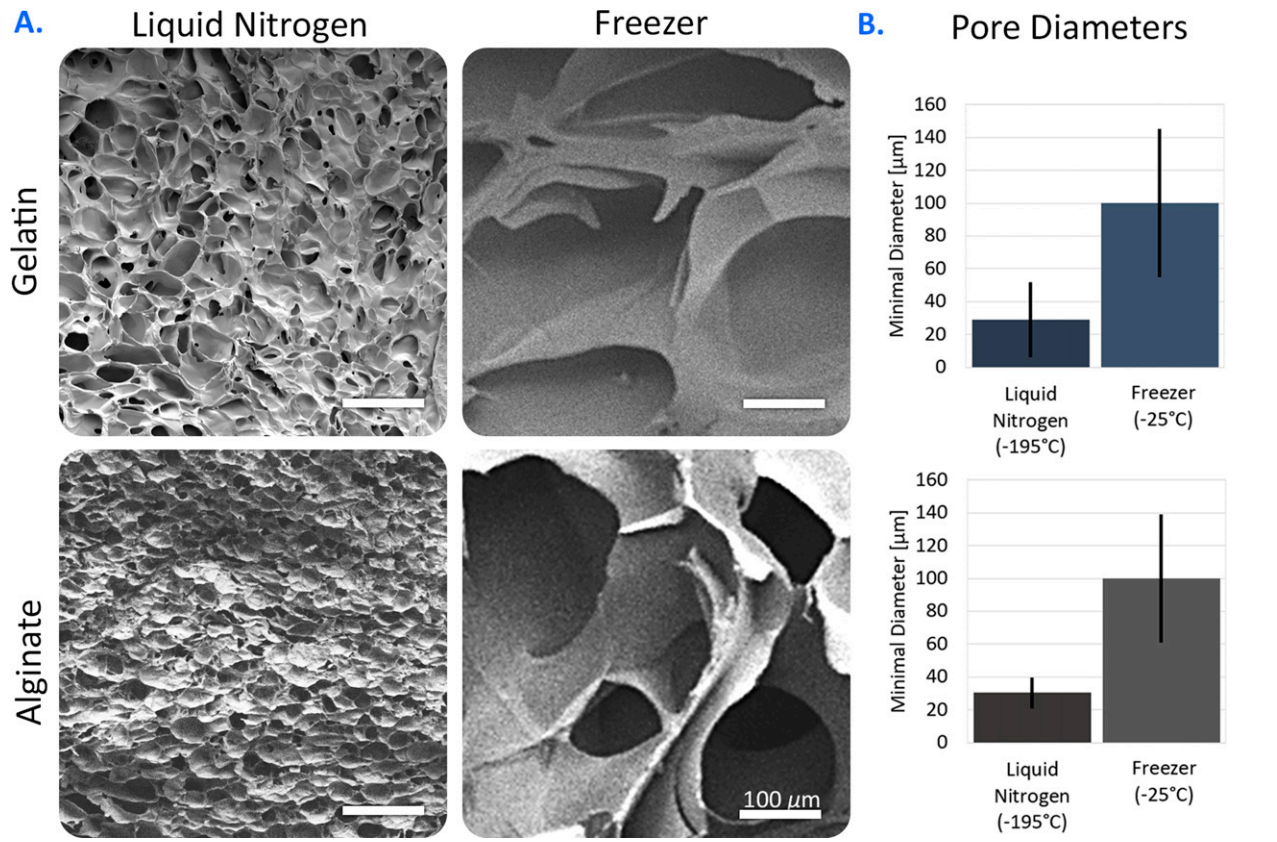

FIG. 4. **(A)** SEM micrographs showing cross-sections of gelatin (*top*) and alginate (*bottom*) hydrogels, frozen either in liquid nitrogen (*left*) or in the freezer (*right*). All images are shown at equal scale. **(B)** Bar graphs show average minimal pore diameters ± standard deviation for gelatin (*top*) and alginate (*bottom*).

barrier. SEM is characterized by such resolution in theory, but it is not the case for hydrogels in practice. Indeed, the vacuum cannot get as good as plenty of water remains in samples even after drying, the sample is not conductive and needs to be coated with a metal layer whose thickness (15 nm in our case) is of the same order of magnitude as the mesh size (estimated to be from 10 to 70 nm for GelMA in literature)[17,18] Moreover, any method that would remove the water from the hydrogel will alter the structure anyway.

To obtain a comprehensive understanding of the structure of native hydrated gels, one must study mesh size through other indirect characterization methods that explore the gel's behavior in its native hydrated state. Mesh size can be estimated using the rubber elasticity theory[5,19] from compression, tensile tests, rheometry, and atomic force microscopy indentation.[15,20] Mesh size can also be estimated using the equilibrium swelling theory.[5,19] Additionally, mesh size can be estimated by diffusion studies, such as fluorescence recovery after photobleaching or diffusion cell setups, exploiting the mesh transport theory.[18,21,22] However, these mathematical models have their own shortcomings, while their inherent assumptions exclude certain types of hydrogels.

Pore size measurements in freeze-dried porous scaffolds

SEM measurements can be relevant when freeze-drying is used willingly to generate pores in the hydrogel. However, measurements acquired through SEM might fail to provide an accurate representation of the pores' true characteristics in the subsequent rehydrated state. Confocal microscopy enables the direct visualization of the actual pore morphology in the hydrated state. Many materials possess inherent autofluorescence, allowing for their observation without any use of dye or fluorescent labeling of the hydrogels, provided that the hydrogel is not too opaque.

The discrepancy between freeze-dried and rehydrated states (see Fig. 3) arises owing to a possible transformation of the pores into different shapes upon rehydration. We demonstrate that the magnitude of this phenomenon can vary greatly depending on the nature of the hydrogel. In the case of gelatin, the difference is such that it is not even clear from our observations that the rehydrated hydrogel still has pores, or if the structures that are observed are just cracks resulting from the pore walls swelling, thereby completely collapsing the pores. In these measurements, it is assumed that the darker fluorescent pixels corresponded to void space. There was no evidence of such a drastic transformation in the case of alginate hydrogels, for which there is a good agreement between the SEM image of the freeze-dried samples and the confocal microscope image of the rehydrated sample (see Fig. 3). It can, however, not be excluded that this phenomenon could potentially happen on a longer timescale or in a different medium. Grenier *et al*. evidenced this phenomenon as well with polysaccharide hydrogels.[1] In any case, based on these results, we would recommend to always evaluate pore morphology upon rehydration for each hydrogel system and to never rely solely on SEM for pore size measurements.

Pore size dependence on the cooling rate

The experiment comparing the structure of freeze-dried scaffolds, frozen using either liquid nitrogen or a regular freezer set at −25°C, provides two extreme case scenarios to illustrate the impact of the cooling rate on the pore size. The cooling rate [K/s] determines pore size because the more supercooled the water is, the more primary nucleation is favored over the growth of the ice grains.[1] Overall, the porous fraction stays the same so this results in a greater number of smaller pores.[1,2] Thus, it is essential to report the applied cooling rate. However, it is not always easy nor scientifically warranted to measure the cooling rate directly or to control it precisely. Nevertheless, at least the cooling method and the thickness of the samples should be noted when generating porous scaffolds by freeze-drying.[4]

Conclusions

Our study emphasizes the limitations of using SEM pore size measurements as the sole basis for inferring properties of native hydrated hydrogels. The observed pores in SEM images are not intrinsic to the native gel matrix but are generated during the freeze-drying process required for sample preparation prior to SEM imaging under vacuum. Consequently, these measurements lead to potentially misleading conclusions. To characterize hydrogel structures in the native hydrated state, efforts should be redirected toward mesh size theory. Despite these limitations, SEM measurements can still be relevant, especially when intentional pore generation through freeze-drying is desired. However, the reported results emphasize the significance of freezing conditions, specifically the cooling rate, in dictating pore size. This observation underscores the importance of reporting cooling rates and controlling freezing conditions in research involving cryogenerated porous scaffolds. Additionally, caution should be taken when using SEM dry pore measurements to predict diffusion and cell growth in rehydrated hydrogel materials, as rehydration can significantly alter their structural properties. In this context, confocal microscopy emerges as a valuable tool, providing the direct visualization of the actual pore morphology in the hydrated state, which is impossible when exploiting SEM images. This is easily applied to hydrogels featuring autofluorescence properties, and transmission images can be exploited as well when this is not the case. As we bridge the gap between materials science and biomedical science communities, our study contributes toward a comprehensive understanding of hydrogel behavior, providing recommendations for researchers seeking accurate insights into hydrogel properties.

Acknowledgments

The authors thank Marie-Christine Eloy for assistance in CLSM, Dr. Delphine Magnin for assistance in SEM, Fatma Nalan Çetin for providing help in elaborating the alginate hydrogel protocols, and Andrea El Haddad for her work in sample preparation and data collection.

Authors' Contributions

A.F.: Conceptualization, investigation, and writing. B.V.D.: Resources and material synthesis. S.V.V.: Supervision, final version approval, and funding acquisition. C.D.-G.: Supervision, final version approval, and funding acquisition.

Data Availability Statement

Scripts are available in supplementary materials. All data are available freely upon request.

Disclosure Statement

The authors declare that there is no conflict of interest regarding the publication of this article.

Funding Information

This project (40007548-GOJ3322N) has received funding from the FWO and F.R.S.-FNRS under the Excellence of Science (EOS) program.

Supplementary Material

Supplementary Data S1

References

1. Grenier J, Duval H, Barou F, Lv P, David B, Letourneur D. Mechanisms of pore formation in hydrogel scaffolds textured by freeze-drying. Acta Biomater 2019;94:195–203; doi: 10.1016/j.actbio.2019.05.070
2. Van Vlierberghe S, Cnudde V, Dubruel P, et al. Porous gelatin hydrogels: 1. Cryogenic formation and structure analysis. Biomacromolecules 2007;8(2):331–337; doi: 10.1021/bm060684o
3. Kaberova Z, Karpushkin E, Nevoralová M, Vetrík M, Šlouf M, Dušková-Smrčková M. Microscopic structure of swollen hydrogels by scanning electron and light microscopies: Artifacts and reality. Polymers (Basel) 2020;12(3):578; doi: 10.3390/polym12030578
4. Aston R, Sewell K, Klein T, Lawrie G, Grøndahl L. Evaluation of the impact of freezing preparation techniques on the characterisation of alginate hydrogels by cryo-SEM. European Polymer Journal 2016;82:1–15; doi: 10.1016/j.eurpolymj.2016.06.025
5. Richbourg NR, Peppas NA. The swollen polymer network hypothesis: Quantitative models of hydrogel swelling, stiffness, and solute transport. Progress in Polymer Science 2020;105:101243; doi: 10.1016/j.progpolymsci.2020.101243
6. Li C, Zhang X, Bao C, et al. Freezing-induced chemical crosslinking to fabricate nanocellulose-based cryogels for efficient bilirubin removal. Separation and Purification Technology 2022;300:121865; doi: 10.1016/j.seppur.2022.121865
7. Yao L, Gao H, Lin Z, et al. A shape memory and antibacterial cryogel with rapid hemostasis for noncompressible hemorrhage and wound healing. Chemical Engineering Journal 2022;428:131005; doi: 10.1016/j.cej.2021.131005
8. Sedlačík T, Nonoyama T, Guo H, et al. Preparation of tough double- and triple-network supermacroporous hydrogels through repeated cryogelation. Chem Mater 2020;32(19):8576–8586; doi: 10.1021/acs.chemmater.0c02911
9. Huang B, Wei X, Chen K, Wang L, Xu M. Bioprinting of hydrogel beads to engineer pancreatic tumor-stroma microtissues for drug screening. Int J Bioprint 2023;9(3):676; doi: 10.18063/ijb.v9i3.676

10. Lee Y, Lee JM, Bae PK, Chung IY, Chung BH, Chung BG. Photo-crosslinkable hydrogel-based 3D microfluidic culture device. ELECTROPHORESIS 2015;36(7–8):994–1001; doi: 10.1002/elps.201400465
11. Lim W, Kim GJ, Kim HW, et al. Kappa-carrageenan-based dual crosslinkable bioink for extrusion type bioprinting. Polymers (Basel) 2020;12(10):2377; doi: 10.3390/polym12102377
12. Han Y, Zeng Q, Li H, Chang J. The calcium silicate/alginate composite: Preparation and evaluation of its behavior as bioactive injectable hydrogels. Acta Biomater 2013;9(11):9107–9117; doi: 10.1016/j.actbio.2013.06.022
13. Tanum J, Udomsom S, Wattanutchariya W, Sooksaen P, Kantawong F. Characterization of gelatin composite with low content hydroxyapatite and the influence on mesenchymal stem cell culture. KEM 2016;675-676:473–476; doi: 10.4028/www.scientific.net/KEM.675-676.473
14. Van Den Bulcke AI, Bogdanov B, De Rooze N, Schacht EH, Cornelissen M, Berghmans H. Structural and rheological properties of methacrylamide modified gelatin hydrogels. Biomacromolecules 2000;1(1):31–38; doi: 10.1021/bm990017d
15. Van Hoorick J, Gruber P, Markovic M, et al. Cross-linkable gelatins with superior mechanical properties through carboxylic acid modification: Increasing the two-photon polymerization potential. Biomacromolecules 2017;18(10):3260–3272; doi: 10.1021/acs.biomac.7b00905
16. Sardelli L, Tunesi M, Briatico-Vangosa F, Petrini P. 3D-reactive printing of engineered alginate inks. Soft Matter 2021;17(35):8105–8117; doi: 10.1039/D1SM00604E
17. Vigata M, Meinert C, Bock N, Dargaville BL, Hutmacher DW. Deciphering the molecular mechanism of water interaction with gelatin methacryloyl hydrogels: Role of ionic strength, pH, drug loading and hydrogel network characteristics. Biomedicines 2021;9(5):574; doi: 10.3390/biomedicines9050574
18. Miri AK, Hosseinabadi HG, Cecen B, Hassan S, Zhang YS. Permeability mapping of gelatin methacryloyl hydrogels. Acta Biomater 2018;77:38–47; doi: 10.1016/j.actbio.2018.07.006
19. Rehmann MS, Skeens KM, Kharkar PM, et al. Tuning and predicting mesh size and protein release from step growth hydrogels. Biomacromolecules 2017;18(10):3131–3142; doi: 10.1021/acs.biomac.7b00781
20. Richbourg NR, Rausch MK, Peppas NA. Cross-evaluation of stiffness measurement methods for hydrogels. Polymer 2022;258:125316; doi: 10.1016/j.polymer.2022.125316
21. Richbourg NR, Peppas NA. High-throughput FRAP analysis of solute diffusion in hydrogels. Macromolecules 2021;54(22):10477–10486; doi: 10.1021/acs.macromol.1c01752
22. Richbourg NR, Ravikumar A, Peppas NA. Solute transport dependence on 3D geometry of hydrogel networks. Macromol Chem Phys 2021;222(16):2100138; doi: 10.1002/macp.202100138

Address correspondence to:
Christine Dupont-Gillain, PhD
Bio and Soft Matter
Institute of Condensed Matter and Nanosciences
Université catholique de Louvain
Place Louis Pasteur 1/L4.01.10
1348 Louvain-la-Neuve
Belgium

E-mail: christine.dupont@uclouvain.be

Received: March 28, 2024
Accepted: June 25, 2024
Online Publication Date: July 4, 2024